Original Article

Experimental Analysis on Machining Properties in Turning of Nimonic C-263

Muhammad Ikhwan Roslim[1], Mohamad Ridzuan Jamli[2], Al Emran Ismail[3], Muhamad Arfauz A Rahman[4]

[1,2]*Faculty of Manufacturing Engineering, Universiti Teknikal Malaysia Melaka, Hang Tuah Jaya, Durian Tunggal, Melaka, Malaysia*
[3]*Faculty of Mechanical and Manufacturing Engineering, Universiti Tun Hussein Onn Malaysia, Batu Pahat, Johor, Malaysia.*
[4]*School of Mechanical and Aerospace Engineering, Queen's University, University Road, Belfast, Northern Ireland, BT7 1NN, United Kingdom.*

[2]*Corresponding Author : ridzuanjamli@utem.edu.my*

Abstract - Due to their exceptional mechanical qualities, nickel-based superalloys are among the ultimate popular materials utilised in the production of aircraft components. Within the family of superalloys, Nimonic C-263 is becoming a challenging material that can be used for manufacturing mechanical components, making it difficult to achieve the appropriate surface roughness as an effect of the alloy's high potential of work hardening, low conductivity of heat, and hot hardness. It is indirect contrast to the fabrication of aeroplane components, which calls for extremely precise machining components to eliminate wastage and scrapping. The current research objective is to ascertain how the tool life is affected by machining parameters during the turning process. Using Titanium Aluminium Nitride, carbide inserts coated with TiAlN to machine Nimonic C-263 alloy in a zero-lubrication cutting condition. Researchers have also evaluated the feed rate, cutting speed, and depth effects on the insert life. The interactions between the output variable and machining parameters investigate using the Box-Behnken technique in Response Surface Methodology (RSM). The agreement between the generated prediction model output and the corresponding variable was accessed using the Analysis of Variance (ANOVA). The findings indicate excellent suitability between the observed and predicted tool life values of 6.9% percentage error against the generated mathematical models.

Keywords - Nimonic C-263, Nickel-based superalloys, Surface Response Methodology, Tool life.

1. Introduction

Nickel (Ni)-based superalloys have recently found a wide range of uses, especially in gas turbines and essential components of aeronautical engines. These alloys are employed in the power plant, aerospace, defence, maritime, and nuclear sectors [1-3]. Nimonic C-263 is more commonly used in the aerospace, defense, and nuclear industries because of its admirable mechanical properties at excellent temperature strength, which include high hardness, tensile strength, thermal fatigue resistance to corrosion, thermal stability, and oxidation [4,5]. They can function effectively even in high-stress environments of long-term and high temperatures. The aerospace industry is one of the forerunners in developing superalloys because more potent and more efficient jet engines will result from the ability of the engine to tolerate greater temperatures [6]. It says that machining this Ni-based superalloy presents several challenges due to its low thermal conductivity at higher temperatures, propensity for work-hardening, and production of abrasive particles in its structure. It typically contains 50% nickel, 20% chromium, and smaller amounts of aluminum, cobalt, and titanium, primarily used in gas turbines and internal combustion engines [7].

Owing to their hot hardness, low thermal conductivity, high work hardening tendency, chemical affinity for tool materials, and the existence of rough carbide particles in their microstructures, these materials present a significant hurdle during machining [5,8]. Nimonic C-263 has higher yield strength and is a low-creep, high-temperature superalloy. Because of its extraordinary properties, including excellent thermal fatigue and creep resistance, Nimonic C-263 is commonly installed in the gas turbine hot combustion area. The machining process of Nimonic C-263 and other Ni-based alloys has garnered much attention because of their reaction tendency with the cutting tool materials, greater strength and increased hardness at high temperatures, and lower thermal diffusivity [7–10]. In the past few years, the main interest of the manufacturing sector has been to maintain a high production rate while meeting

the customer demands for high-quality machining practices, particularly concerning the use of Ni-based superalloy materials [13].

Cutting temperature, power consumption, tool wear, chip morphology, surface roughness, and cutting force are output parameters that influence Ni-based alloy machining performance. These characteristics have an impact on surface integrity, corrosion resistance, fatigue strength, and dimensional precision, which are the fundamental requirements that need to be possessed by any metal alloy before being used in the aerospace industry [7]. As a difficult-to-machine material and significantly impacts the alloy's machinability, plastic deformations are easier to form in the machining of Nimonic C-263. This results from the observed higher cutting temperature, viscosity, cutting force, significant tool wear, and the degree of hardening process [14]. Furthermore, higher temperatures reduce machining efficiency and increase processing costs owing to increasing tool wear.

The degree of tool wear is often measured in terms of its life, where it is the period a tool may be used efficiently for machining before it has to be replaced or regrind. It depends on the type of material used to make the tool and the cutting conditions [15]. Machining cost, cutting power, and friction influence machining quality in the cutting process. After surpassing a certain threshold, tool wear will initiate cutting temperature increment, vibration, and cutting force, thus diminishing surface integrity and dimension inaccuracy outside the tolerance range [16].

The cutting tool failure mechanism is connected to the simultaneous activities at the rake surface and the flank surface. Since adhesion, abrasion, and plastic deformation all work together to cause flank wear, the tool material must be strong enough to withstand this wear. Abrasive wear is the predominant mechanism of flank wear [17]. In addition to rapid tool failure, Built-Up Edges (BUE) and burrs are commonly produced in machining alloys. BUE eliminates tool material when it slides off due to its instability, causing the tool substrate to chip and crack. [18]. The main cause of crater development or surface wear on rakes is diffusion, in addition to the adhesion and abrasion forces from chips and swarf across the rake surface [22]. When examining tool life, the fundamental criterion for determining a tool's superiority over other tools is flank wear. The tool's diffusion wear, oxidation wear, adhesion wear, and mechanical wear become more severe during the Ni-based superalloys machining process, rising a constrained tool life [27]. Among other principal tool wear in Ni-based super alloys machining process is the built-up layer formation on the cutting tool surface, notching, abrasion flank wear and crater [2].

The main concern of obtaining longer tool life is to produce acceptable surface roughness. The surface roughness can have a substantial influence on the tribological properties of the surface. The degree of roughness influences the interaction of a real object with its surroundings. Rough surfaces generally have high friction coefficients and wear more quickly than smooth surfaces [19]. Because of the significant association between machined component performance and manufacturing cost, surface integrity database and tool life within specific machining conditions are frequently critical to designers and manufacturers [26].

Ezilarasan et al. [21] studied the interactions between surface finish, cutting force and tool wear in the dry machining of Nimonic C-263. The whisker-reinforced ceramic insert was used as the cutting tool, and the main contributor to the flank wear progression was the feed rate rather than the cutting speed. Velmurugan et al. [14] also found that the cutting depth and feed rate contribute to higher cutting force in the dry cutting process of Nimonic C-263 utilising a Physical Vapor Deposition (PVD) coated insert. On the other hand, abrasive wear was identified to be dominating the wear mechanism for the PVD-coated insert during the Nimonic C-263 cutting process, as found by several researchers [8,22].

From the literature, it can be concluded that tool life is one of the crucial influences that affect the cutting quality of Nimonic C-263, and most of the studies concentrated on the tool wear without varying feed rate, as well as cutting depth. Furthermore, studies on the tool life in the Nimonic C-263 cutting process are still inadequate. Consequently, the present research is aimed to produce a prediction model in the dry-cutting process of Nimonic C-263 with several combinations of cutting parameters.

2. Methodology

Nimonic C-263 alloy rods, 120 mm in length and 91 mm in diameter, were purchased; their average hardness was 32 HRC. The alloys showed the following chemical composition- 48.06% Nickel (Ni), 20.08% Chromium (Cr), 19.52% Cobalt (Co), 6.82% Molybdenum (Mo), 2.88% Carbon (C), 2.19% Titanium (Ti) and 0.44% Silicon (Si). As seen in Fig. 1**,** the primary elements in the alloy were Nickel (Ni) and Chromium (Cr).

CNC Lathe Haas ST-2 was employed to perform the turning process in dry conditions. The parameters considered in this study were – the rate of feed (f), depth of cut (DOC), and cutting Speed (Vc). The target functions were considered to be tool wear (Vb). Three turning factors were used in the study. Table 1 below shows the different combinations of DOC, f, and Vc employed in the experiments.

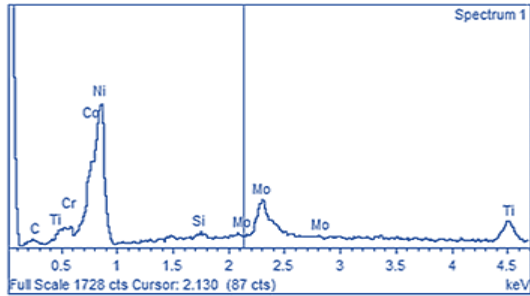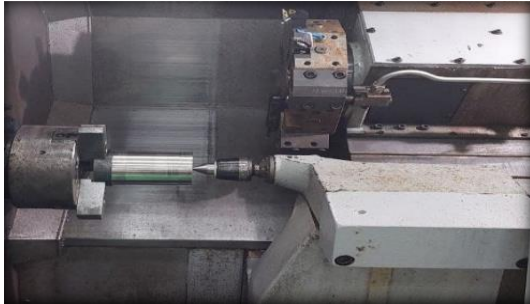**Fig. 1 Composition of Nimonic C-263**

Fig. 2 Experimental Setup

Table 1. Experimental parameters

Parameter	Depth of Cut (DOC)	Rate of Feed (f)	Cutting Speed (Vc)
Level/unit	mm	mm/rev	m/min
Low	0.3	0.05	60
Medium	0.4	0.10	90
High	0.5	0.15	120

Because of its many advantages in the fields of validation, design, and control of machining processes, modelling is regarded as the most commonly used technique during the machining processes. Instead of costly and time-consuming trials, numerical simulations in machining may be used to predict materials and equipment's thermal and mechanical behaviour. The input values affect the accuracy of all results simulated in the experiments. Hence, it is crucial to comprehend how the input data influence the prediction of the simulated outputs.

Predictive models of machining processes can help determine and assess the machining performance indicators like cutting forces, chip formation, tool wear, cutting temperature, and surface finish [9]. A design matrix was developed using the RSM experimental setup based on a few carefully selected parameters. Various combinations of all parameters (such as DOC, f, and V_c.) were employed in the design. According to the Box-Behnken technique, the design had 17 rows, which equated to the total number of experimental trials.

In the turning experiments, the cutting tools used were PVD-coated (AlTiN) carbide inserts. These cutting tools had a rhombic shape and included a chip breaker and ISO code (CNGG 120408-SGF 1105) for carbide tips. The cutting tool holder was based on the DCLNR 2020K12 specification.

A Mitutoyo tool maker microscope was used to measure flank wear, while Scanning Electron Microscope (SEM) was used to observe the wear mechanism. The average wear, denoted by V_b and maximum wear land size V_{bmax}, is used to calculate flank wear. The cutting experiment tool wear criteria was average flank wear, $V_b \geq$ 0.2 mm, considering the experimentation duration and material consumption, cutting-edge fracture, severe flaking and excessive chipping. At the cutting intervals of 20 mm cutting distance, tool wear was measured. After the flank wear reaches $V_b \geq$ 0.2 mm, the cutting tool will be put under the SEM machine to analyse the wear mechanism present on the cutting tool.

3. Results and Discussion

The RSM technique combined all the parameters and generated a design summary. RSM is seen as a statistical and mathematical approach to modelling, analysing, and improving all processes. The machining properties were predicted using RSM, and this model could also be useful for predicting the values of all the selected attributes before conducting the actual experimentation [27]. ANOVA interaction and potential influencing parameters/variables can both be examined using the RSM technique. The model's applicability is assessed using the ANOVA, which is also used to examine how machining parameters affect response. This response surface methodology (RSM) is crucial for the planning, designing, formulating, developing, and analysis of the new technique [21].

Additionally, it has the ability to enhance already completed studies and products. RSM cover a body method that combines statistical and mathematical approaches to find the best-operating conditions using experimental methods. The experiments were carried out utilising Box-Behnken based on a mix of parameters produced by RSM analysis. RSM frequently combine factorial design techniques with Box-Behnken and central composite designs. RSM was used in design optimisation to reduce the cost of pricy analysis methods and their associated numerical noise [24]. 17 trial runs were performed, and RSM was used to design and develop the combination factor. Using ANOVA, the influence of each parameter on the PVD-coated (AlTiN) carbide inserts tool life was investigated.

3.1. Tool Wear Progression

Table 2 below shows the experimental result of tool life in dry machining according to the Box-Behnken technique.

Table 2. Experimental result

Trial No.	Control Factors			Mean Responses Value
	f (mm/rev)	V_c (m/min)	DOC (mm)	Tool life (min)
1	0.10	60.00	0.30	15.41
2	0.10	120.00	0.30	2.58
3	0.15	90.00	0.30	5.37
4	0.10	90.00	0.40	7.03
5	0.15	90.00	0.50	6.01
6	0.10	60.00	0.50	15.22
7	0.10	90.00	0.40	6.17
8	0.10	90.00	0.40	5.4
9	0.05	90.00	0.50	8.81
10	0.10	120.00	0.50	1.86
11	0.15	60.00	0.40	8.8
12	0.05	60.00	0.40	28.75
13	0.10	90.00	0.40	5.7
14	0.10	90.00	0.40	6.47
15	0.15	120.00	0.40	1.21
16	0.05	120.00	0.40	3.48
17	0.05	90.00	0.30	8.28

Fig. 3 Wear progression at Run 15

Fig. 4 Measured wear progression according to cutting distance

Fig. 3 depicts the tool wear progression with cutting parameters of DOC = 0.4 mm, V_c = 120 m/min and f = 0.05 mm/rev. The tool could barely move 80 mm above cutting parameters before suffering a catastrophic failure. The V_b measured at the initial stage at a 20 mm distance was 0.036 mm. A uniform wear rate was noted in the middle stage. As depicted in Fig. 4, the wear and tear of the component confine to the cutting tool's tip. During the last stages of machine wearing, the wear rate increased dramatically. At a distance of 60 mm, the recorded value of V_b was 0.089 mm, whereas, at a distance of 80 mm, a fracture at the flank face occurred with a recorded V_b value of 0.202 mm.

It highlights the existence of rapid tool wear. The tool was completely worn and ruined due to its blunted state upon machining. This phenomenon will impact the cutting tool's performance and its geometry. A similar result was noted by Sulaiman et al. [25], indicating a rapid increase in wear rate with the increment of cutting speed, and flank wears accelerate more quickly at a maximal cutting speed. Cutting temperature and pressure increment placed on the cutting edge would result in an increase in cutting speed [3].

Fig. 5 below shows the lowest cutting speed of the experiment, which is 60 m/min; the tool managed to travel up to 320 mm in the length of the machining. This was the highest recorded distance travelled by the PVD-coated insert in the experiments. Following the feed rate at 0.05 mm/rev and 0.4 mm depth of cut, the Vb value recorded at the early stage of the first 20 mm distance, the V_b value recorded was 0.025 mm. The uniform wear rate is observed in Fig. 6 below until it reaches the V_b wear rate value of 0.201 mm at a 320 mm distance.

3.2. Material Removal Rate Analysis
3.2.1. 1200 mm³/min
Fig. 7 illustrates the flank wear morphologies obtained from SEM machine analysis at Run 12. The flank face was fractured, which was caused to the high stress, and periodic vibration was applied directly at the cutting edge throughout the machining of Ni-based alloys. A fatal failure is further worsened by the concentration of stress near the cutting edge. The flank face exhibits adhesion as well. Adhesion, also known as the cold-welding phenomenon, is a phenomenon that results from the plastic deformation of the workpieces under adequate temperature and pressure conditions. The adhesive forces induce it among atoms that develop on the frictional contact surface. When the grains or groups of grains were removed by shear or tension, in addition to the relative motion of the adhesion sites on two friction surfaces, adhesive wear occurred. Under high pressure and high-temperature conditions, an adhesion layer was pushed into the newly produced micro cracks. As a result, the crack was propagated and extended along the lateral axis, worsening the tool wear and fracture failure.
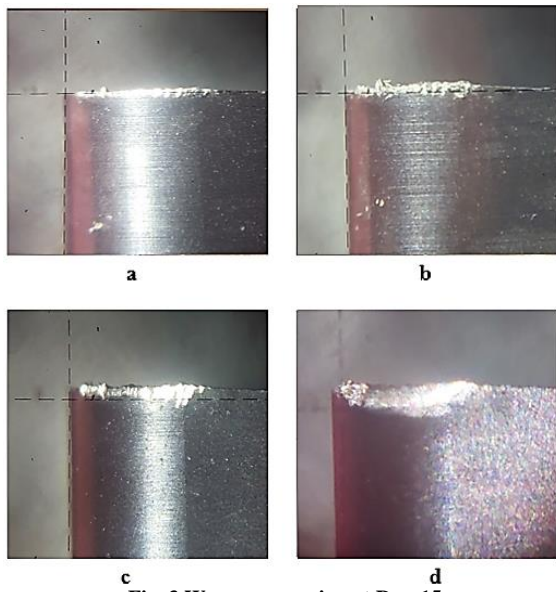
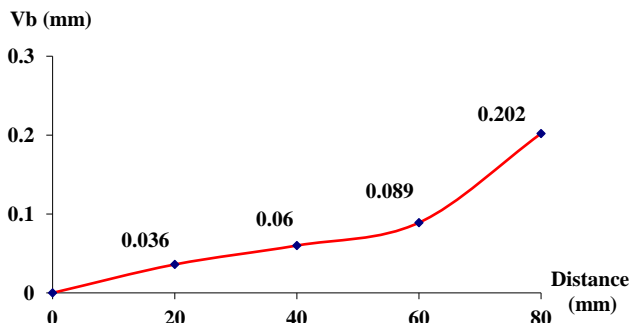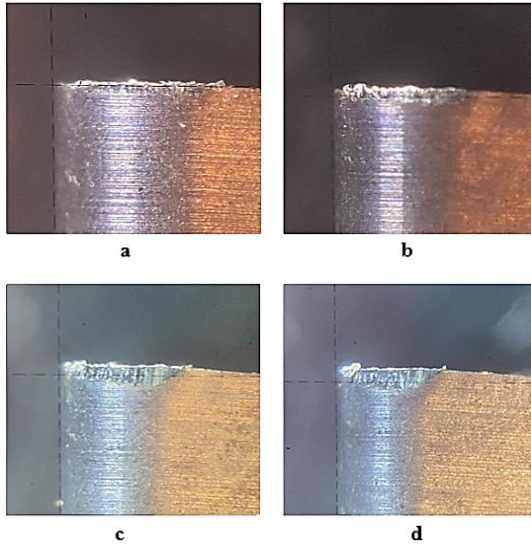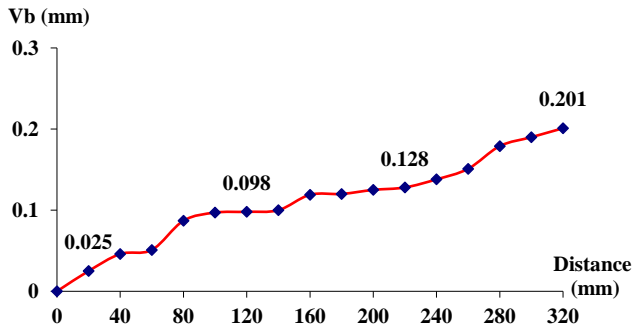**Fig. 5 Wear progression at Run 12**

Fig. 6 Measured wear progression according to cutting distance

During the dry turning of the superalloys, the cutting edge underwent intense alternating stress, where the distribution and concentration of the stress gradient may lead to the development of micro cracks.

3.2.2. 3600 mm³/min

Fig. 8 displays the flank wear morphologies determined by the SEM machine analysis at Run 13. The study found that the adhesion process and tool temperature significantly impacted BUE formation. The BUE formation was visible on the cutting-edge notch zone and tool nose.

3.2.3. 7200 mm³/min

Fig. 9 depicts the morphologies of flank wear obtained from SEM machine analysis at Run 15. The scratches on the worn surface were evident, suggesting an abrasive wear mechanism. The relative mobility of specific trapped rigid inclusions or worse asperities at contact with the surface often generates abrasive wear. The mechanical loading pushes the rigid inclusions into the friction surface, where sliding friction and abrasive ploughing generate trough-shaped indentations. When dry-turning Ni-based superalloys, the adhesive layer is present throughout the whole cutting process and instantly displays scratch effects when mechanical loading is applied. The rigid inclusions scrape the flank face of the workpiece in the same direction as the movement of the workpiece. With a decrease in the peel-off frequency of the adhesive layer, the clarity of the scratches increases and eventually causes abrasive wear.
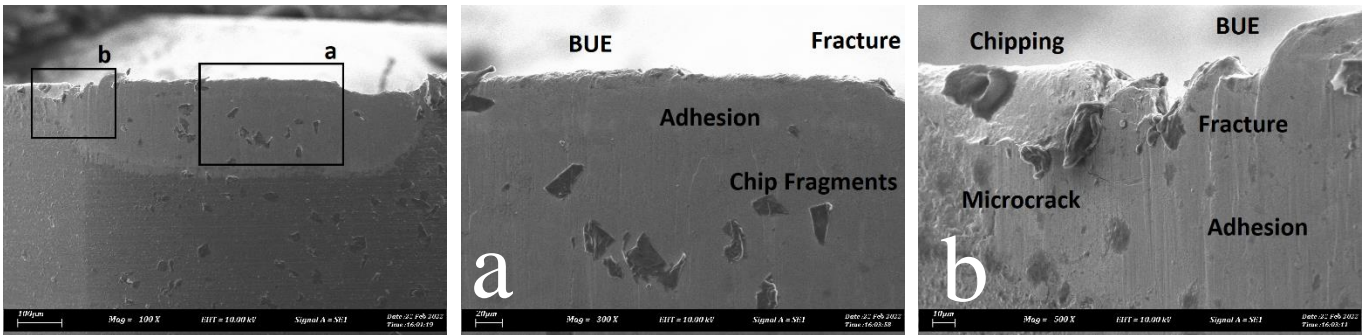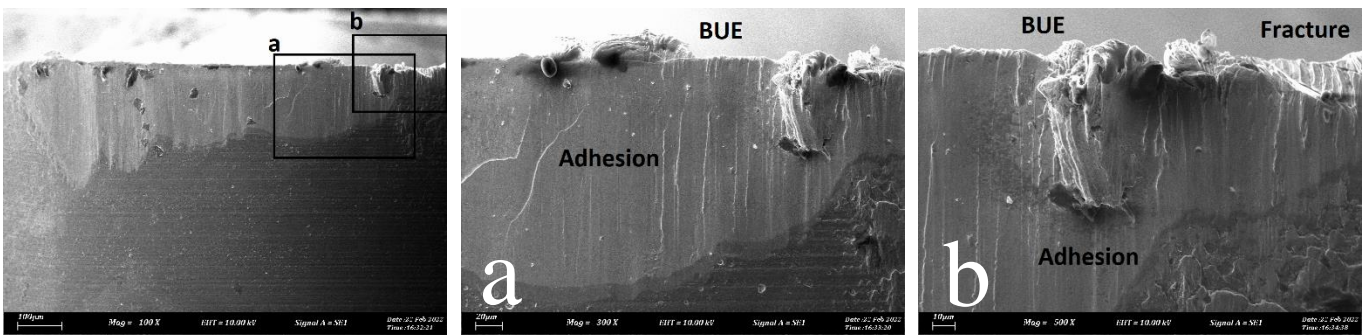

Fig. 7 Flank face at MRR: 1200 mm³/min, Vb:0.201mm
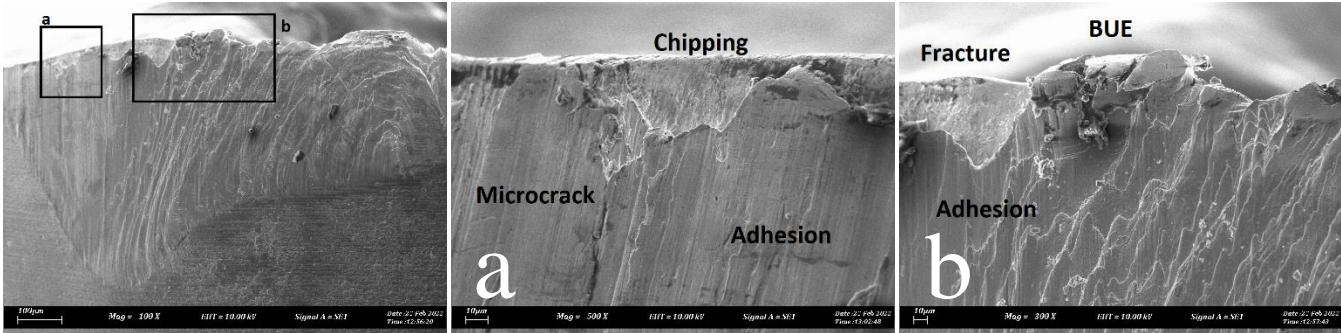

Fig. 8 Flank face at MRR: 3600 mm³/min, Vb:0.204mm

Fig. 9 Flank face at MRR: 7200 mm3/min, Vb:0.202mm
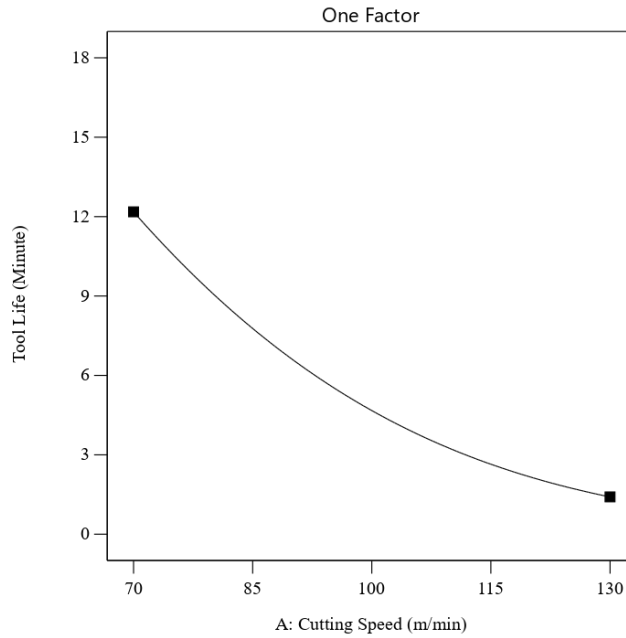
Fig. 10 The influence of cutting speed on tool life
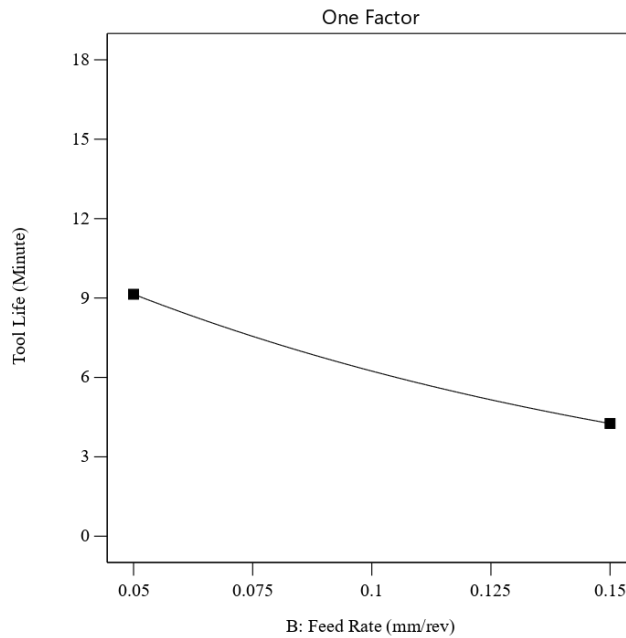
Fig. 11 The influence of feed rate on tool life
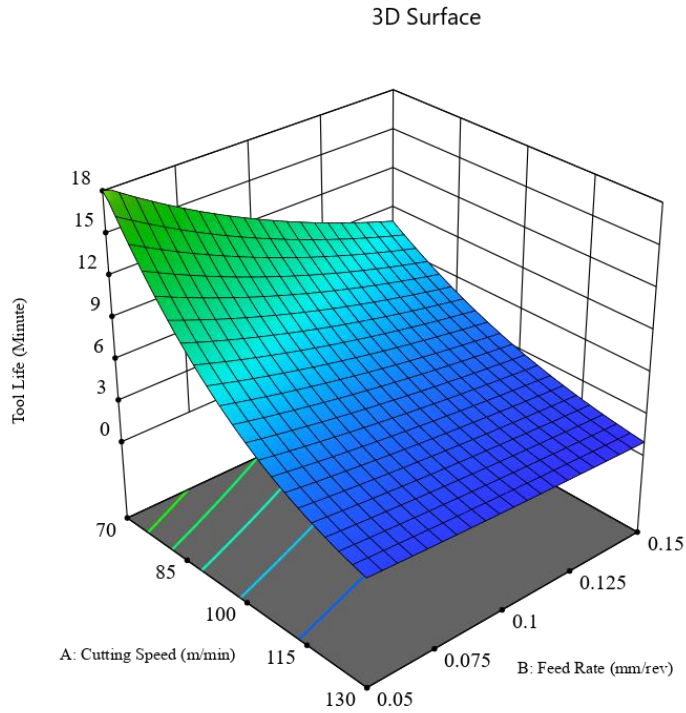
Fig. 12 Tool life 3D response

Table 3. ANOVA Analysis

Source	Sum of Squares	df	Mean Square	p-value	F-value	
Model	9.21	5	1.84	< 0.0001	50.94	significant
A-cutting speed	7.97	1	7.97	< 0.0001	220.52	
B-Rate of Feed	1.17	1	1.17	0.0001	32.30	
C-Cutting Depth	0.0034	1	0.0034	0.7647	0.0941	
AB	0.0041	1	0.0041	0.7437	0.1124	
A²	0.0611	1	0.0611	0.2200	1.69	
Lack of Fit	0.3545	7	0.0506	0.0768	4.70	not significant
Residual	0.3976	11	0.0361			
Pure Error	0.0431	4	0.0108			
Cor Total	9.60	16				

3.3. ANOVA Analysis for Tool Life

Tool wear is recognised as a significant feature of machinability, with a direct or indirect impact on several performance measures. It is defined as the crater and flank wear visible under an optical microscope following the machining process. Tool life can be calculated based on the accumulated flank wear. The results presented in Table 3. indicate that V_c directly impacts tool life.

The findings shown in Fig. 10, Fig. 11 and Fig. 12 indicate a decrease in tool life alongside the feed rate and cutting speed rise. The tool wear progression is categorised into three major stages which are an early stage, wherein there is a high level of flank wear increment, a stable stage, wherein there is a gradual flank wear increment, which directs to the development of flaking and notch wear near, and a final stage wherein the tool wear showed a catastrophic failure.

3.4. Mathematical Model Validation

A validation experiment was carried out at a randomly selected parameter value to validate the mathematical model equation generated by ANOVA. The value is located between the range of cutting depth, 0.3 to 0.5 mm, cutting speed, 60 to 120 m/min, and 0.05 to 0.15 mm/rev feed rate.

The regression model was developed to evaluate tool life as given in equations (1). The tool life model equation's value compares the tool life acquired from experimental data.
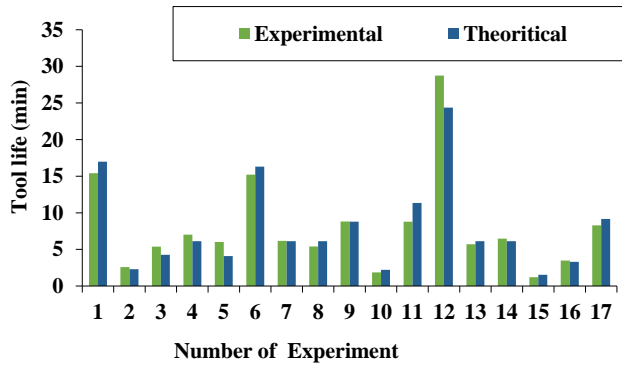
Fig. 13 Tool life value from experiment, minutes

$$ln(toollife) = 4.82054 - 0.011368(A) - 9.55155(B)$$
$$- 0.206222(C)$$
$$+ 0.021246(AB) - 0.000133(A^2) \quad (1)$$

Where:
A: Cutting speed
B: Rate of feed
C: Cutting Depth

Fig. 13 compares the experimental data of tool life with the theoretical data derived from the developed mathematical model. The comparison indicates that the predicted values are closer to the experimental value. Parameters like V_c and f significantly affected the tool life, wherein cutting implemented at their highest values resulted in rapid tool wear increment, as seen in Run 10 and Run 15. On the other hand, the highest tool life was noted in Run 12. The results showed that the highest tool life was noted at the lowest cutting speed and feed rate, as in Runs 1 and 6.

The cutting parameter for the validation studies is tabulated in Table 5. The tool life value was derived using equation 1. The validation test results are provided in Table 6 below. According to Table 6, the measured tool life value varies inside the projected optimal range of the various responses, where the confidence interval of the validation studies was 95.86%.

Table 4. Estimator of statistical model accuracy

	R-squared	Standard deviation	Adj. R-squared
Tool life (min)	0.9586	0.1901	0.9398

Table 5. Validation test cutting parameter

Factors	Cutting Speed (m/min)	Feed Rate (mm/rev)	Depth of Cut (mm)
Value	100	0.07	0.45

Table 6. Validation test result

	Predicted (DOE)	Experimental	Percentage Error (%)
Value	5.7033	5.31	6.9

The experiment's error percentage was 6.9%, as indicated. The value also matched the experimental data and the predicted values, less than 10%. Therefore, the mathematical model result of the optimal process input parameter for the response was validated as the percentage error was less than 10%.

4. Conclusion

The Response Surface Methodology (RSM) was used to predict the output response values based on the input parameters involved in the machining of Ni-based alloy, namely Nimonic C-263, in no lubrication condition. The mathematical model that was generated showed a significantly suitable output parameter validated using the Box-Behnken design.

Various mathematical models were developed using the RSM process to establish a link between the input factors (cutting depth, cutting speed, and rate of feed) and output response. ANOVA was used to confirm the model's suitability and the accuracy of its associated variables. This research concludes that:

- The RSM-generated mathematical model is validated, and the validation results showed a <10% of percentage error.

- The maximum tool life for the PVD-coated carbide insert was 28.75 mins, while the minimal tool life was 1.21 mins. Cutting speed during the machining process significantly affected the tool life, followed by the cutting depth and rate of feed.

- The SEM approach provided more insight into the failure mechanisms of the cutting tools used in the Nimonic C-263 superalloy cutting process. Adhesion was seen as the primary wear mechanism at an MRR of 1200 mm^3/min, while fracture was the primary failure mechanism. Furthermore, at MRR of 7200 mm^3/min, the major wear mechanisms were severe adhesion and diffusion, while cutting-edge microchipping and micro-cracks were the predominant failure mechanisms. This discrepancy can be attributable to the various alternating main effects applicable during the heat softening and strain hardening mechanisms underlying the various cutting speed situations.

Acknowledgments

References

[1] Aruna Thakur, Soumya Gangopadhyay, Aveek Mohanty and Kalipada Maity, "Experimental Assessment on Performance of Tin / Ticn / Al 2 O 3 / Zrcn Coated Tool During Dry Machining of Nimonic C-263," *Journal of Machining,* vol. 18, no.5-6, pp. 452–465, 2016. Crossref, https://doi.org/10.1504/IJMMM.2016.078985

[2] G. Nasr, M. Soltantarzeh, B. Davoodi, and A. Hajaliakbari, "Assessment of Tool Wear Mechanisms in High-Pressure Jet-Assisted Turning Process of a Nickel-Based Superalloy," *Wear*, vol. 460–461, no. 8, pp. 203454, 2020. Crossref, https://doi.org/10.1016/j.wear.2020.203454

[3] C. Xue and W. Chen, "Adhering Layer Formation and its Effect on the Wear of Coated Carbide Tools During Turning of a Nickel-Based Alloy," *Wear*, vol. 270, no. 11–12, pp. 895–902, 2011. Crossref, https://doi.org/10.1016/j.wear.2011.02.018

[4] F. Wang, J. Liu, and Q. Shu, "Milling Wear of Carbide Tool for Processing Nickel-Based Alloy in Cryogenic Based on the Entropy Change," *The International Journal of Advanced Manufacturing Technology*, vol. 90, no. 5–8, pp. 1703–1713, 2017. Crossref, https://doi.org/10.1007/s00170-016-9505-4

[5] A. Thakur and S. Gangopadhyay, "International Journal of Machine Tools & Manufacture State-of-the-Art in Surface Integrity in Machining of Nickel-Based Super Alloys," *International Journal of Machine Tools and Manufacture*, vol. 100, pp. 25–54, 2016. Crossref, https://doi.org/10.1016/j.ijmachtools.2015.10.001

[6] A. Kale and N. Khanna, "A Review on Cryogenic Machining of Super Alloys Used in Aerospace Industry," *Procedia Manufacturing*, vol. 7. pp. 191–197, 2017. Crossref, https://doi.org/10.1016/j.promfg.2016.12.047

[7] P. S. Jadhav, C. P. Mohanty, T. K. Hotta, and M. Gupta, "An Optimal Approach for Improving the Machinability of Nimonic C-263 Superalloy During Cryogenic Assisted Turning," *Journal of Manufacturing Processes*, vol. 58, no. 8, pp. 693–705, 2020. Crossref, https://doi.org/10.1016/j.jmapro.2020.08.017

[8] B. Koyilada, S. Gangopadhyay, and A. Thakur, "Comparative Evaluation of Machinability Characteristics of Nimonic C-263 Using CVD And PVD Coated Tools," *Journal of the International Measurement Confederation*, vol. 85, pp. 152–163, 2016. Crossref, https://doi.org/10.1016/j.measurement.2016.02.023

[9] D. Ulutan and T. Ozel, " Machining Induced Surface Integrity in Titanium and Nickel Alloys : A Review," *International Journal of Machine Tools and Manufacture*, vol. 51, no. 3, pp. 250–280, 2011. Crossref, https://doi.org/10.1016/j.ijmachtools.2010.11.003

[10] L. Tu, W. Ming, X. Xu, C.Cai, J.Chen, Q.An, J.Xu and M. Chen, "Wear and Failure Mechanisms of Sialon Ceramic Tools During High-Speed Turning of Nickel-Based Superalloys," *Wear*, vol. 488–489, no. 10, pp. 204171, 2022. Crossref, https://doi.org/10.1016/j.wear.2021.204171

[11] G. R. Thellaputta, P. S. Chandra, and C. S. P. Rao, "ScienceDirect 5th International Conference of Materials Processing and Characterization (ICMPC 2016) Machinability of Nickel Based Superalloys : A Review," *Materials Today: Proceedings*, vol. 4, no. 2, pp. 3712–3721, 2017. Crossref, https://doi.org/10.1016/j.matpr.2017.02.266

[12] Y. Li, B. Zou, Z.Shi, C. Huang, L. Li, H. Liu, H. Zhu, P. Yao and J. Liu, "Wear Patterns and Mechanisms of Sialon Ceramic End-Milling Tool During High Speed Machining of Nickel-Based Superalloy," *Ceramics International*, vol. 47, no. 4, pp. 5690–5698, 2021. Crossref, https://doi.org/10.1016/j.ceramint.2020.10.155

[13] A. R. Choudhury, R. Kumar, A. K. Sahoo, A. Panda and A. Malakar, "Machinability Investigation on Novel Incoloy 330 Super Alloy Using Coconut Oil Based Sio2 Nano Fluid," *International Journal of Integrated Engineering,* vol. 12, no. 4, pp. 145–160, 2020. Crossref, https://doi.org/10.30880/ijie.2020.12.04.014

[14] K. V. Velmurugan, K. Venkatesan, S. Devendiran and A. T. Mathew, "Dry Machining of Nimonic 263 Alloy Using PVD and CVD Inserts," Springer, *Singapore*, 2018. Crossref, https://doi.org/10.1007/978-981-13-2718-6_18

[15] M. Sunday Abolarin, O. Oluwafemi Ayodeji, J. Jonathan Yisa, P. Solomon Olaoluwa and A. Clement Kehinde, "Effect of Cutting Speed and Feed Rate on Tool Wear Rate and Surface Roughness in Lathe Turning Process," *International Journal of Engineering Trends and Technology*, vol. 22, no. 4, pp. 171–173, 2015. Crossref, https://doi.org/10.14445/22315381/IJETT-V22P236

[16] V. Patidar, K. Gangrade, and S. Sharma, "Wear Analysis of Multi Point Milling Cutter using FEA," *International Journal of Engineering Trends and Technology*, vol. 47, no. 6, pp. 336–343, 2017. Crossref, https://doi.org/10.14445/22315381/IJETT-V47P254

[17] K. Senthil Kumar and J. S. Senthil Kumar, "Analysis of Flank Wear and Chip Morphology When Machining Super Duplex Stainless Steel in a Gas Cooled Environment," *International Journal of Engineering and Technology*, vol. 5, no. 6, pp. 5045-5056, 2013.

[18] B. Davoodi and B. Eskandari, "Tool Wear Mechanisms and Multi-Response Optimisation of Tool Life and Volume of Material Removed in Turning of N-155 Iron-Nickel-Base Superalloy using RSM," *Journal of the International Measurement Confederation*, vol. 68, pp. 286–294, 2015. Crossref, https://doi.org/10.1016/j.measurement.2015.03.006

[19] J. M. Zhou, H Persson, Z Chen, R M Saoubi, D Gustafsson, V Bushyla, V Akujarvi, J.E Stahl and R Peng, "Surface Characterisation of AD730TM Part Produced in High Speed Turning with CBN tool," *Procedia CIRP*, vol. 71, pp. 215–220, 2018. Crossref, https://doi.org/10.1016/j.procir.2018.05.068

[20] Nandkumar N. Bhopale and Datttatraya. S. Pimpalgaonkar, "A Study on the Machinability Characteristics of Superalloys Inconel-718 during High-Speed Milling," *SSRG International Journal of Mechanical Engineering*, vol. 8, no. 2, pp. 1-7, 2021. Crossref*,* https://doi.org/10.14445/23488360/IJME-V8I2P101

[21] C. Ezilarasan, V. S. Senthil Kumar, and A. Velayudham, "An Experimental Analysis and Measurement of Process Performances in Machining of Nimonic C-263 Super Alloy," *Journal of the International Measurement Confederation*, vol. 46, no. 1, pp. 185–199, 2013. Crossref*,* https://doi.org/10.1016/j.measurement.2012.06.006

[22] A. Singh, S. Ghosh, and S. Aravindan, "Flank Wear and Rake Wear Studies for Arc Enhanced Hipims Coated Altin Tools During High Speed Machining of Nickel-Based Superalloy," *Surface and Coatings Technology*, vol. 381, pp. 125190, 2020. Crossref*,* https://doi.org/10.1016/j.surfcoat.2019.125190

[23] G.T.Suriyaprabakaran, M.Kavin and R.Govindaraj, "Analyzing The Effect of Machining Parameters For Titanium (Grade 5) Alloy," *SSRG International Journal of Material Science and Engineering,* vol. 6, no. 2, pp. 9-22, 2020. Crossref, https://doi.org/10.14445/23948884/IJMSE-V6I2P102

[24] P. Qiu, M. Cui, K.Kang, B.Park, Y. Son, E. Khim, M. Jang and J. Khim, "Application of Box-Behnken Design with Response Surface Methodology for Modeling and Optimising Ultrasonic Oxidation of Arsenite with H 2O2," *Central European Journal of Chemistry*, vol. 12, no. 2, pp. 164–172, 2014. Crossref, https://doi.org/10.2478/s11532-013-0360-y

[25] S. H. Y. and M. R. S. M.A. Sulaiman, M.S. Asiyah, R. Shahmi, R. Zuraimi, E. Mohamad and M.S. Salleh, "Cryogenic as Alternative Cooling Method during Turning Titanium Alloy : A International Conference on Design and Concurrent Engineering 2017 Cryogenic as Alternative Cooling Method during Turning Titanium Alloy : A Review," *International Conference on Design and Concurrent Engineering 2017 & Manufacturing Systems Conference,* no. 10, 2017.

[26] M. A. İnce and İ. Asiltürk, "Effects of Cutting Tool Parameters on Surface Roughness," *International Refereed Journal of Engineering and Science,* vol. 4, no. 8, pp. 15–22, 2015.

[27] J. Francis Xavier, B. Ravi, D. Jayabalakrishnan, C. Ezilarasan, V. Jayaseelan, and G. Elias, "Experimental Study on Surface Roughness and Flank Wear in Turning of Nimonic C263 under Dry Cutting Conditions," *Journal of Nanomaterials*, vol. 2021, 2021. Crossref, https://doi.org/10.1155/2021/2054399